Original Paper

Explainable Machine Learning Techniques To Predict Amiodarone-Induced Thyroid Dysfunction Risk: Multicenter, Retrospective Study With External Validation

Ya-Ting Lu[1], MS; Horng-Jiun Chao[1], BS; Yi-Chun Chiang[1,2], PhD; Hsiang-Yin Chen[1,2], MS, PharmD

[1]Department of Clinical Pharmacy, School of Pharmacy, Taipei Medical University, Taipei, Taiwan

[2]Department of Pharmacy, Wan Fang Hospital, Taipei Medical University, Taipei, Taiwan

Corresponding Author:
Hsiang-Yin Chen, MS, PharmD
Department of Clinical Pharmacy
School of Pharmacy
Taipei Medical University
R714, 7th Floor, Health and Science Building No.250
Wuxing Street, Xinyi Distict
Taipei, 110
Taiwan
Phone: 886 2 2736 1661 ext 6175
Fax: 886 2 2736 1661
Email: shawn@tmu.edu.tw

Abstract

Background: Machine learning offers new solutions for predicting life-threatening, unpredictable amiodarone-induced thyroid dysfunction. Traditional regression approaches for adverse-effect prediction without time-series consideration of features have yielded suboptimal predictions. Machine learning algorithms with multiple data sets at different time points may generate better performance in predicting adverse effects.

Objective: We aimed to develop and validate machine learning models for forecasting individualized amiodarone-induced thyroid dysfunction risk and to optimize a machine learning–based risk stratification scheme with a resampling method and readjustment of the clinically derived decision thresholds.

Methods: This study developed machine learning models using multicenter, delinked electronic health records. It included patients receiving amiodarone from January 2013 to December 2017. The training set was composed of data from Taipei Medical University Hospital and Wan Fang Hospital, while data from Taipei Medical University Shuang Ho Hospital were used as the external test set. The study collected stationary features at baseline and dynamic features at the first, second, third, sixth, ninth, 12th, 15th, 18th, and 21st months after amiodarone initiation. We used 16 machine learning models, including extreme gradient boosting, adaptive boosting, k-nearest neighbor, and logistic regression models, along with an original resampling method and 3 other resampling methods, including oversampling with the borderline-synthesized minority oversampling technique, undersampling–edited nearest neighbor, and over- and undersampling hybrid methods. The model performance was compared based on accuracy; Precision, recall, F_1-score, geometric mean, area under the curve of the receiver operating characteristic curve (AUROC), and the area under the precision-recall curve (AUPRC). Feature importance was determined by the best model. The decision threshold was readjusted to identify the best cutoff value and a Kaplan-Meier survival analysis was performed.

Results: The training set contained 4075 patients from Taipei Medical University Hospital and Wan Fang Hospital, of whom 583 (14.3%) developed amiodarone-induced thyroid dysfunction, while the external test set included 2422 patients from Taipei Medical University Shuang Ho Hospital, of whom 275 (11.4%) developed amiodarone-induced thyroid dysfunction. The extreme gradient boosting oversampling machine learning model demonstrated the best predictive outcomes among all 16 models. The accuracy; Precision, recall, F_1-score, G-mean, AUPRC, and AUROC were 0.923, 0.632, 0.756, 0.688, 0.845, 0.751, and 0.934, respectively. After readjusting the cutoff, the best value was 0.627, and the F_1-score reached 0.699. The best threshold was able to classify 286 of 2422 patients (11.8%) as high-risk subjects, among which 275 were true-positive patients in the testing set. A shorter treatment duration; higher levels of thyroid-stimulating hormone and high-density lipoprotein cholesterol; and lower levels of free thyroxin, alkaline phosphatase, and low-density lipoprotein were the most important features.

Conclusions: Machine learning models combined with resampling methods can predict amiodarone-induced thyroid dysfunction and serve as a support tool for individualized risk prediction and clinical decision support.

(J Med Internet Res 2023;25:e43734) doi: 10.2196/43734

KEYWORDS

amiodarone; thyroid dysfunction; machine learning; oversampling; extreme gradient boosting; adverse effect; resampling; thyroid; predict; risk

Introduction

Amiodarone-induced thyroid dysfunction (AITD) is a common, irreversible, and unpredictable adverse thyroid effect, leading to therapy failure and significant mortality. As it is the drug of choice for arrhythmias and atrial fibrillation, developing predictive models for the early detection of AITD is warranted [1-4]. The incidence of AITD varies with iodine intake and ranges from 17% to 30% [5-7]. Studies indicate that AITD onset is unpredictable [8], and it is followed by significant morbidity and mortality [9]. Amiodarone has a long and variable half-life of approximately 60 to 142 days [10-14], causing difficulty in treating its side effects. Timely and precise patient stratification to identify patients at high risk of AITD is the foremost strategy for preventing life-threatening adverse thyroid effects.

Predicting AITD requires advanced data-mining skills to unveil its multifactorial mechanisms. Older age, female sex, chronic obstructive pulmonary disease, chronic kidney disease, and underlying autoimmune thyroid disorders contribute to AITD [6,15-22]. Previously, statistical approaches were used to develop a risk prediction index for AITD for adults with congenital heart disease [23] and to perform an AITD risk factor analysis [24-26]. However, these studies failed to capture dynamic factors, as they collected data at a single time point. A limited sample size, heterogeneous patient cohort, single data-collection time point, and lack of consideration of factorial interactions further contributed to suboptimal predictive performance. In another report, a machine learning algorithm was used to study immune checkpoint inhibitor–induced thyroid dysfunction and was found to have an area under the receiver operating characteristic curve (AUROC) of 0.77 [27]. This model outperformed conventional regression models for predicting multiple diseases, such as hypertension [28], neck pain [29], and hepatocellular carcinoma [30]. The robust nature of machine learning techniques could be promising for building a surveillance system for AITD in comparison to traditional regression methods.

Combining machine learning and resampling strategies can counteract imbalanced data resulting from the low incidence of AITD in the real world. Tree-based ensemble learning methods, such as extreme gradient boosting (XGBoost) and adaptive boosting (AdaBoost), are commonly applied for imbalance classification [31,32]. K-nearest neighbors (KNN) with data resampling methods perform well in imbalance classification [33]. Combined with the synthetic minority oversampling technique (SMOTE), these methods rebalance the minority and achieve promising performance in disease and survival prediction [34,35]. Borderline SMOTE further improves internal data distribution by using samples on the boundary to synthesize new instances and is able to diagnose lung cancer early [36]. Edited nearest neighbor (ENN) removes ambiguous data from the majority class, while borderline synthetic minority oversampling technique–edited nearest neighbor (B-SMT-ENN) is a hybrid technique that performs oversampling by SMOTE and undersampling by ENN. These hybrid sampling methods successfully improve adverse-effect predictions and have other medical applications [37-39].

An accurate machine learning prediction model with a resampling strategy can be applied to overcome imbalanced data for multifactorial adverse effects. The objectives of this study were to develop and validate machine learning models for forecasting individualized AITD risk with imbalanced real-world data. The performance of 12 models with 4 machine learning classifiers, including XGBoost, AdaBoost, KNN, and logistic regression (LR), along with 3 resampling methods (borderline-SMOTE, ENN, and B-SMT-ENN), were compared. The specific aims of this study were (1) to select a fine-tuned model for AITD prediction with multiple performance metrics, including accuracy; Precision, recall, F_1-score, G-mean, AUROC, and AUPRC, and (2) to optimize machine learning-based risk stratification schemes for AITD by readjusting the decision thresholds for individualized risk prediction.

Methods

Ethical Considerations

This retrospective study used a delinked clinical research database from 3 hospitals in the Taipei Medical University health care system, including Taipei Medical University Hospital, Wan Fang Hospital, and Shuang Ho Hospital. The study was approved by the Taipei Medical University Joint Institutional Review Board (N202107054). As the data were deidentified, the requirement for informed consent was waived. This study adhered to the TRIPOD (Transparent Reporting of a Multivariate Prediction Model for Individual Prognosis or Diagnosis) checklist [40].

Study Design

Figure 1 shows the study design, including data collection, feature selection, model construction, and 5-fold internal validation using a training set, external validation by a test set, and model interpretation. The training set of the study comprised patients from Wan Fang Hospital and Taipei Medical University Hospital, whereas the external test set comprised patients from Shuang Ho Hospital. There were 16 machine learning models built by the training set. Model performance was compared with the external testing set.

Figure 1. Study design to construct machine learning models for predicting amiodarone-induced thyroid dysfunction. The test set performance was evaluated in the same sequence as the training set. The green boxes indicate that the validation process was completed. Ada: adaptive boosting; AUPRC: area under the precision-recall curve; B-SMT: oversampling with borderline synthetic minority oversampling technique (borderline SMOTE); ENN: edited nearest neighbor (ENN); G-mean: geometric mean; Hyb: hybrid oversampling with borderline synthetic minority oversampling technique and undersampling with edited nearest neighbor (B-SMT-ENN); KNN: k-nearest neighbor; LR: logistic regression; SHAP: Shapley additive explanations; SHH: Shuang Ho Hospital; SMT: synthetic minority oversampling technique; TMUCRD: Taipei Medical University clinical research database; TMUH: Taipei Medical University Hospital; WFH: Wan Fang Hospital; XGB: extreme gradient boosting.

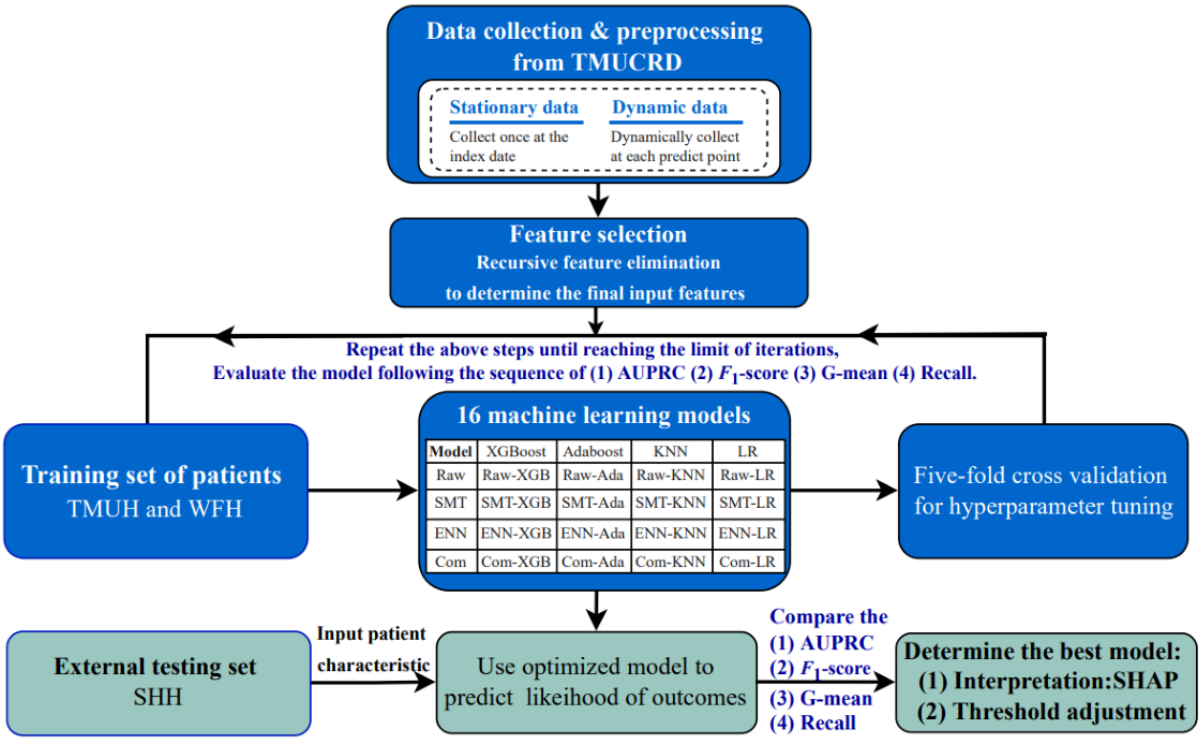

Patient Cohort

Patients older than 18 years who had first been prescribed oral amiodarone between January 2005 and December 2017 were included. Patients were excluded if they were pregnant or had a history of a thyroid disorder diagnosis, thyroid surgery, or subclinical thyroid laboratory data (Multimedia Appendix 1) within 1 year before the index day, which was the day of the first amiodarone prescription. The predefined inclusion and exclusion criteria were modified from previous medication-induced thyroid dysfunction research [6,27]. The study subjects were followed up for 2 years after the index date. This study collected features until the end of the study period and recorded patient loss to follow-up and the occurrence of AITD events.

Data Collection and Preprocessing

The study collected stationary and dynamic features from the clinical research database. Stationary features, including sex, age, and BMI, were collected once at the index date. Dynamic features, including laboratory tests, comorbidities, and comedications, were continuously collected to reflect the patient's clinical condition. The collection points for dynamic features were at baseline and the first, second, third, sixth, ninth, 12th, 15th, 18th, and 21st months after amiodarone initiation. Details of the dynamic data collection are shown as a diagram in Multimedia Appendix 2. The features reengineered by the research team included the accumulated or average dose of amiodarone and annual time-series variations in laboratory tests. Robust scaler algorithms were used to normalize the data and reduce the effect of extreme numeric variables and large differences in range between laboratory values [41]. Variables with more than 90% missing data were deleted from the machine learning programs. Missing values were first imputed with the last observation carried forward, and then the remainders were imputed with Multivariate Imputation by Chained Equations (Scikit-learn), an open-source imputation software package [42-44]. Zero was imputed for laboratory data with changing rates, such as the trend or slope of lab values. The codebook and missing rates in the training and test sets are provided in Multimedia Appendix 3.

Dynamic Prediction of the Study Outcome

The outcome for prediction in this study was the occurrence of AITD, which was defined by a thyroid function test and with diagnostic criteria from previous studies [6,22,26,45]. Cases of AITD were identified if the thyroid-stimulating hormone (TSH) titer was <0.1 mU/l and the free thyroxin (fT4) level was higher than the normal range, while cases of amiodarone-induced hypothyroidism were ascertained by a serum TSH titer of >10 mU/l, regardless of the fT4 level; a TSH titer of 4 to 10 mU/l with a lower than normal fT4 level; an International Classification of Diseases (ICD)-9 code 242, 243, or 244 or an ICD-10 code E02, E03, E05, or E06; having received pharmacotherapy (eg, levothyroxine; Propylthiouracil, carbimazole, or methimazole) for thyroid disease; or an ICD-9 procedure code for a thyroidectomy. As TSH and fT4 are definite diagnostic criteria for AITD, the last data values before

the prediction point were masked to avoid data leakage in the test set. Once a patient developed AITD, the data at that time point were coded 1, and it was designated the earliest AITD onset date.

Model Construction With the Training Data Set

Hyperparameter tuning of the XGBoost, AdaBoost, KNN, and LR algorithms was performed with an exhausted-grid search toward maximizing F_1-score metrics. Five-fold cross-validation was performed inside each grid option, and the optimal hyperparameter set was chosen based on the model in the grid search with the highest F_1-score. XGBoost was tuned on 7 hyperparameters, including *max_depth*, *min_child_weight*, *gamma*, *subsample*, *colsample_bytree*, *n_estimators*, and *learning_rate* for 94,080 grid options. Three hyperparameters of AdaBoost that were tuned included *n_estimators*, *learning rate*, and *algorithm*, with 160 combinations. As the KNN is based on the KNN of the prediction point, *n_neighbors*, *weights*, and *metric*, combining 120 sets of parameters, were tested. Finally, the study used an LR established with the *scikit-learn* module for binary outcome classification. *P Penalty*, *solvers*, and *C*, hyperparameters of LR, were calculated in 140 selections. Details of the hyperparameters and the final best combination of the above 16 models are shown in Multimedia Appendix 4.

Recursive feature elimination (RFE) with cross-validation was used for the training set. Pseudocodes of the grid search and cross-validation are presented in Multimedia Appendix 5. The minimal number of feature sets was generated by XGBoost and AdaBoost. As the incidence of AITD in the training and test sets was 14.3% and 11.4%, respectively, the imbalance issue was managed by (1) oversampling with the borderline synthetic minority oversampling technique (B-SMT) [46]; (2) undersampling the majority class with ENN [47]; and (3) a combination of oversampling and undersampling with B-SMT-ENN. The raw strategy and 3 resampling strategies were applied to XGBoost, AdaBoost, KNN, and LR, as shown in Figure 1. This study finally constructed 16 models through the 5-fold cross-validation process of the training sets.

Model Performance Comparison by Test Set

The performance of the 16 models generated with the training data set were validated and evaluated on the test data set. Model performance was compared using accuracy; Precision, recall, F_1-score, geometric mean, AUROC, and AUPRC [48]. The AUPRC, G-mean, and F_1-score were major metrics over AUROC due to the imbalanced data in this study [49,50]. The study also prioritized recall over precision as the major performance index, to minimize the cost of failing to detect AITD [51], while the accuracy; Precision, and AUROC were minor indices. The formulas of each evaluation metric are provided in Multimedia Appendix 6.

Feature Importance, Threshold Adjustment, and Kaplan-Meier Analysis

This study further analyzed individualized feature importance and survival curves of different thresholds to assess risk factors and differentiate high-risk patients. The Shapley additive explanations (SHAP) python package was used to understand the importance and influence of each risk factor that caused AITD [52]. The contribution of each feature was computed and plotted to interpret the model. The precision-recall (PR) curve of the best model was plotted to determine the optimal cutoff based on the maximum F_1-score. A threshold-moving system was further used by placing different cutoff points on the PR curve for binary classification. Five cutoff points were selected for analysis, including the points to forecast the top 1%, 5%, 15%, and 25% of patients with AITD risk, as well as the one determined by the threshold with the maximized F_1-score [53]. The recall and sensitivity for the above 5 cutoff points were then calculated and compared. A Kaplan-Meier (KM) survival curve was plotted using different cutoff thresholds to compare the actual survival of high- and low-risk groups for statistical comparison.

Statistical Analysis

Baseline characteristics were evaluated with the chi-square test or Fisher exact test for categorical variables, and independent 2-tailed *t* tests were used for continuous variables. The Wilcoxon rank-sum test was used when the data were not normally distributed. The cumulative thyroid dysfunction incidence was compared with the log-rank test. Data were analyzed using SAS (version 9.4; SAS Institute); Python (version 3.9.5; Python Software Foundation), and R studio (version 1.3.1093; R Studio). The statistical significance of the AUPRC was calculated using MedCalc (MedCalc Software).

Results

Baseline Characteristics

The study included 6497 amiodarone users. The results of a univariate analysis of their demographics and other features are shown in Table 1. The Strengthening The Reporting of Observational Studies in Epidemiology (STROBE) flowchart for patient selection is presented in Multimedia Appendix 7. The training set contained 4075 subjects, among whom 583 (14.3%) developed AITD, while the test set had 2422 patients, among whom 275 (11.35%) had AITD. The distribution of gender and mean age did not significantly differ between the training and test sets. The AITD group had a higher proportion of female patients, and its median age was older than that of the non-AITD group.

Table 1. Patient demographics and univariate analysis.

Characteristics	Training set (N=4075)			Test set (N=2422)		
	AITD[a] (n=583, 14.3%)	Non-AITD (n=3492)	*P* value	AITD (n=275, 11.4%)	Non-AITD (n=2147)	*P* value
Patient demographics						
Male, n (%)	282 (48.37)	1969 (56.38)	<.001	121 (44)	1214 (56.54)	<.001
Age (years), median (IQR)	76.00 (66.00-83.00)	73.00 (62.00-83.00)	.001	75.00 (64.00-83.00)	72.00 (61.00-81.00)	.006
BMI (kg/m^2), median (IQR)	24.14 (21.83-26.67)	24.27 (22.04-26.50)	.75	24.94 (22.83-27.04)	24.49 (22.22-26.51)	.02
Charlson comorbidity index, median (IQR)	1.00 (1.00-2.00)	1.00 (1.00-2.00)	.79	1.00 (0.00-1.00)	1.00 (1.00-2.00)	.003
Smoking habit, n (%)	11 (1.89)	56 (1.6)	.75	0 (0)	17 (0.79)	.27
Alcohol habit, n (%)	11 (1.89)	63 (1.8)	>.99	3 (1.09)	38 (1.77)	.57
Indication for amiodarone, n (%)						
Atrial fibrillation	360 (61.75)	223 (38.25)	<.001	178 (64.73)	1192 (55.52)	.004
Supraventricular tachycardia	95 (16.3)	509 (14.58)	.29	28 (10.18)	321 (14.95)	.04
Use of amiodarone, median (IQR)						
Cumulative dose (g)	18.20 (5.60-39.00)	16.80 (5.00-48.60)	0.49	15.60 (5.60-35.20)	11.60 (3.00-35.00)	.08
Duration (days)	126.00 (28.00-332.00)	115.00 (25.00-554.00)	.02	125.00 (28.00-290.00)	75.00 (15.00-442.00)	.64
Prescription daily dose (mg/day)	200.00 (134.09-217.02)	200.00 (136.36-261.91)	.04	200.00 (127.88-216.13)	200.00 (141.61-238.89)	.16
Average dose per kg body weight (g/kg)	0.30 (0.09-0.62)	0.27 (0.08-0.75)	.64	0.24 (0.08-0.55)	0.18 (0.05-0.55)	.08
Laboratory data, median (IQR)						
Thyroid-stimulating hormone (mU/l)	3.20 (2.79-3.51)	2.08 (1.40-2.50)	<.001	3.22 (2.97-3.40)	2.13 (1.45-2.50)	<.001
Free thyroxine (ng/dl)	1.18 (1.11-1.25)	1.27 (1.17-1.39)	<.001	1.16 (1.10-1.21)	1.22 (1.10-1.31)	<.001
High-density lipoprotein cholesterol (mg/dL)	55.03 (47.93-60.39)	53.00 (45.49-59.99)	.001	53.00 (44.00-58.33)	50.64 (40.00-57.32)	.16
Low-density lipoprotein cholesterol (mg/dL)	89.29 (79.00-101.49)	91.72 (80.45-106.31)	.001	90.00 (81.00-101.00)	92.22 (81.00-110.00)	.12
Red blood cells (10^6 cells/μL)	4.21 (3.57-4.42)	4.23 (3.60-4.48)	.06	4.25 (3.66-4.47)	4.24 (3.66-4.51)	.67
Hemoglobin (g/L)	12.80 (11.00-13.40)	12.87 (10.90-13.60)	.05	12.80 (11.20-13.50)	12.90 (11.10-13.70)	.31
Hematocrit (%)	37.9 (32.7-39.6)	38.3 (32.7-40.21)	.007	38.18 (33.2-40)	38.35 (33.2-40.6)	.35
Alkaline phosphatase (U/L)	64.68 (53.66-83.07)	75.85 (60.29-96.00)	<.001	58.70 (47.26-78.10)	75.42 (58.92-95.38)	<.001
Triglycerides (mg/dl)	86.00 (72.60-119.00)	91 (74.00-124.00)	.02	84.60 (73.86-118.00)	92.00 (76.00-132.00)	.02
Concurrent medication, n (%)						
Allopurinol	30 (5.14)	110 (3.15)	.02	9 (3.27)	88 (4.1)	.62
Tyrosine kinase inhibitors	1 (0.17)	38 (1.08)	.04	1 (0.36)	9 (0.41)	>.99
Nonsteroidal anti-inflammatory drugs	218 (37.39)	1135 (32.5)	.02	90 (32.73)	814 (37.91)	.11
Diabetes mellitus medications	133 (22.81)	638 (18.27)	.01	47 (17.09)	393 (18.3)	.68
Metformin	94 (16.12)	450 (12.89)	.04	29 (10.54)	287 (13.37)	.22
Concurrent diseases, n (%)						

Characteristics	Training set (N=4075)			Test set (N=2422)		
	AITD[a] (n=583, 14.3%)	Non-AITD (n=3492)	*P* value	AITD (n=275, 11.4%)	Non-AITD (n=2147)	*P* value
Hypertension	415 (71.18)	2275 (65.14)	.005	171 (62.18)	1278 (59.52)	.44
Bradycardia	22 (3.77)	68 (1.94)	.009	6 (2.18)	23 (1.07)	.19
Diabetes	210 (36.02)	1068 (30.58)	.01	77 (28)	698 (32.51)	.15
Anemia	94 (16.12)	435 (12.46)	.02	26 (9.45)	254 (11.83)	.29
Gout	79 (13.55)	338 (9.67)	.005	20 (7.27)	157 (7.31)	>.99
Chronic renal failure	113 (19.3)	548 (15.69)	.03	32 (11.63)	292 (13.6)	.42
Renal dysfunction	174 (29.83)	786 (22.51)	<.001	54 (19.64)	459 (21.38)	.56

[a]AITD: amiodarone-induced thyroid dysfunction.

Model Construction and Evaluation

Feature selection by RFE with 5-fold cross-validation generated 19 features with an accuracy of 0.895 with AdaBoost, while 46 features with an accuracy of 0.914 were generated by XGBoost. Considering the simplicity and accuracy of the model, the 19 features selected by AdaBoost were used for further model development. A figure showing RFE and the features selected is provided in Multimedia Appendix 8.

Figure 2 compares the major model performance indices for the test set: AUPRC, F_1-score, G-mean, and recall. The internal validation performance of the training set is provided in Multimedia Appendix 9. The 4 major performance metrics for the XGBoost and AdaBoost models were consistently higher than for the KNN and LR models, with higher AUPRC and F_1-scores for the XGBoost-based model. Among different resampling methods, the best AUPRC was for XGBoost-B-SMT (0.751, 95% CI 0.697-0.799), which was significantly higher than for XGBoost-Raw (0.742, 95% CI 0.687-0.790; P<.05), XGBoost-ENN (0.741, 95% CI 0.686-0.790; P<.05), and XGBoost-B-SMT-ENN (0.730, 95% CI 0.675-0.779; P<.05). Multimedia Appendix 10 summarizes the results of the statistical comparisons for AUPRCs.

Figure 2. Performance metrics for evaluating a model on imbalanced data. AdaBoost: adaptive boosting; AUPRC: area under the precision-recall curve; B-SMT: borderline synthesized minority oversampling technique; B-SMT ENN: hybrid oversampling with borderline synthetic minority oversampling technique and undersampling with edited nearest neighbor; ENN: edited nearest neighbor.

XGBoost-based models also produced higher G-means, with values of 0.688, 0.661, and 0.641 for XGBoost-B-SMT, XGBoost-ENN, and XGBoost-B-SMT-ENN, respectively. The 3 resampling methods all increased G-mean performance for XGBoost and AdaBoost but did not consistently increase the G-mean for KNN or LR. Finally, the recall levels of XGBoost-B-SMT and AdaBoost-B-SMT reached 0.756 and 0.858, respectively, while KNN-ENN only rounded to 0.255.

Table 2 further lists the performance on all metrics, including the minor indices of accuracy; Precision, and AUROC, for the test sets. All models had an AUROC >0.8, except the LR model without resampling. Like the major metrics, the AdaBoost- and XGBoost-based models had higher accuracy and AUROC values compared to the KNN- and LR-based models. The AUROC values for the XGBoost- and AdaBoost-based models were >0.9, while only the accuracy of the XGBoost-based models exceeded 0.9.

Table 2. Model performance to predict amiodarone-induced thyroid dysfunction.

Models	Major indices				Minor indices		
	AUPRC[a]	Recall	F_1-score	G-mean[b]	Accuracy	Precision	AUROC[c]
XGBoost[d]							
Raw	0.742	0.607	0.670	0.769	0.932	0.748	0.936
B-SMT[e]	0.751	0.756	0.688	0.845	0.923	0.632	0.934
ENN[f]	0.741	0.702	0.661	0.815	0.918	0.624	0.939
B-SMT ENN[g]	0.730	0.673	0.641	0.797	0.914	0.611	0.924
AdaBoost[h]							
Raw	0.643	0.516	0.593	0.708	0.919	0.696	0.923
B-SMT	0.654	0.858	0.589	0.861	0.864	0.448	0.921
ENN	0.635	0.742	0.640	0.829	0.905	0.562	0.922
B-SMT ENN	0.624	0.822	0.583	0.847	0.867	0.452	0.914
K-nearest neighbor							
Raw	0.500	0.149	0.249	0.385	0.898	0.759	0.835
B-SMT	0.470	0.829	0.330	0.699	0.617	0.206	0.816
ENN	0.393	0.255	0.337	0.496	0.886	0.496	0.825
B-SMT ENN	0.467	0.822	0.338	0.709	0.635	0.213	0.813
Logistic regression							
Raw	0.294	0.073	0.118	0.26	0.877	0.313	0.798
B-SMT	0.303	0.804	0.377	0.742	0.698	0.246	0.806
ENN	0.300	0.229	0.260	0.462	0.852	0.300	0.811
B-SMT ENN	0.305	0.778	0.389	0.746	0.722	0.259	0.803

[a]AUPRC: area under the precision-recall curve.

[b]G-mean: geometric mean.

[c]AUROC: area under the receiver operating characteristic curve.

[d]XGBoost: extreme gradient boosting.

[e]B-SMT: borderline synthesized minority oversampling technique.

[f]ENN: edited nearest neighbors.

[g]B-SMT ENN: hybrid oversampling with borderline synthetic minority oversampling technique and undersampling with edited nearest neighbor.

[h]AdaBoost: adaptive boosting.

Feature Importance, Threshold Adjustment, and KM Survival Analysis

Figure 3 shows the SHAP summary plot. As shown in this graph, the TSH level had the highest contribution to AITD risk, with a SHAP value of 1.68. The fT4 level, amiodarone treatment duration, alkaline phosphatase level, high-density lipoprotein (HDL) level, and low-density lipoprotein (LDL) level were associated with a higher predicted probability of AITD, with respective SHAP values of 0.95, 0.76, 0.73, 0.52 and 0.37. Furthermore, therapeutic days, cumulative dose, age, and BMI, with SHAP values of 0.45, 0.41, 0.33, and 0.25, respectively, were important global predictors. The local explanation summary plot demonstrated the direction of relationships between clinical variables and AITD, with positive SHAP values indicating higher AITD risk. A higher TSH level was the most informative feature in determining AITD, with a lower fT4 level, shorter treatment duration, lower alkaline phosphatase level, higher HDL level, and lower LDL level increasing the AITD risk. In addition, longer therapeutic days, higher cumulative dose, older age, and lower BMI also raised the AITD risk.

Figure 3. Shapley additive explanations importance plot of the extreme gradient boosting–borderline synthetic minority oversampling technique model. SHAP: Shapley additive explanations.

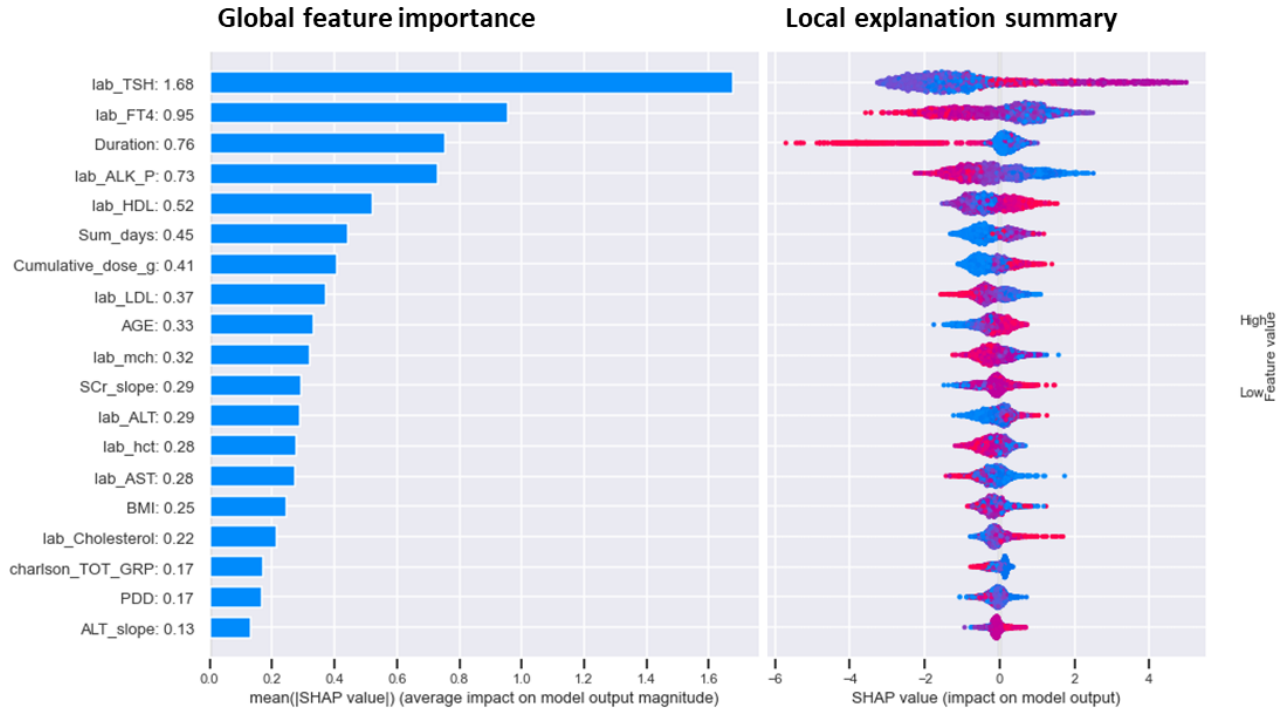

Figure 4 shows KM curves based on using different cutoff points on the PR curve for the XGBoost–borderline SMOTE model. The thresholds of the 5 cutoff points were 0.995 for the top 1% (point A), 0.953 for the top 5% high-risk patients (point B), 0.627 for the optimal point determined by the maximized F_1-score (point C), 0.5 for the top 15% as the default value (point D), and 0.142 for the top 25% (point E) of patients predicted to be at risk of AITD. Moving from default point D, with a threshold of 0.5, to point A, with a threshold of 0.995, the recall significantly decreased from 0.756 to 0.116. When changing the threshold from 0.5 (default; Point D) to 0.142 (point E), recall increased from 0.756 to 0.88. The optimal cutoff (point C), with a threshold of 0.627, yielded better performance, with an accuracy of 0.93 and a precision of 0.685, and the best F_1-score was achieved at 0.699. The corresponding KM curves for the 5 cutoff points were able to differentiate high- and low-risk patients in the log-rank test (P<.001). Point A had only 33 within 2422 patients (1.4%) in the high-risk group, and point E predicted 617 within 2422 patients (25.4%) at high risk of AITD. Point C, with 286 high-risk patients within 2422 patients (11.8%), demonstrated an optimal prediction of 275 true positives for patients with AITD.

Figure 4. Dynamic and interactive threshold-moving system. The figure represents the contribution of the corresponding features to amiodarone-induced thyroid dysfunction risk. Global feature importance refers to a single ranking of all features for the model, while the local explanation calculated Shapley additive explanation values for each prediction to understand features that contributed to that single prediction. The Kaplan-Meier plot of each threshold is shown in the figure. The yellow star represents the optimal cutoffs for threshold, F_1-score, recall, and precision: 0.627, 0.699, 0.713, and 0.685, respectively. AP: average precision; NPV: negative predictive value; PPV: positive predictive value; PR: precision-recall.

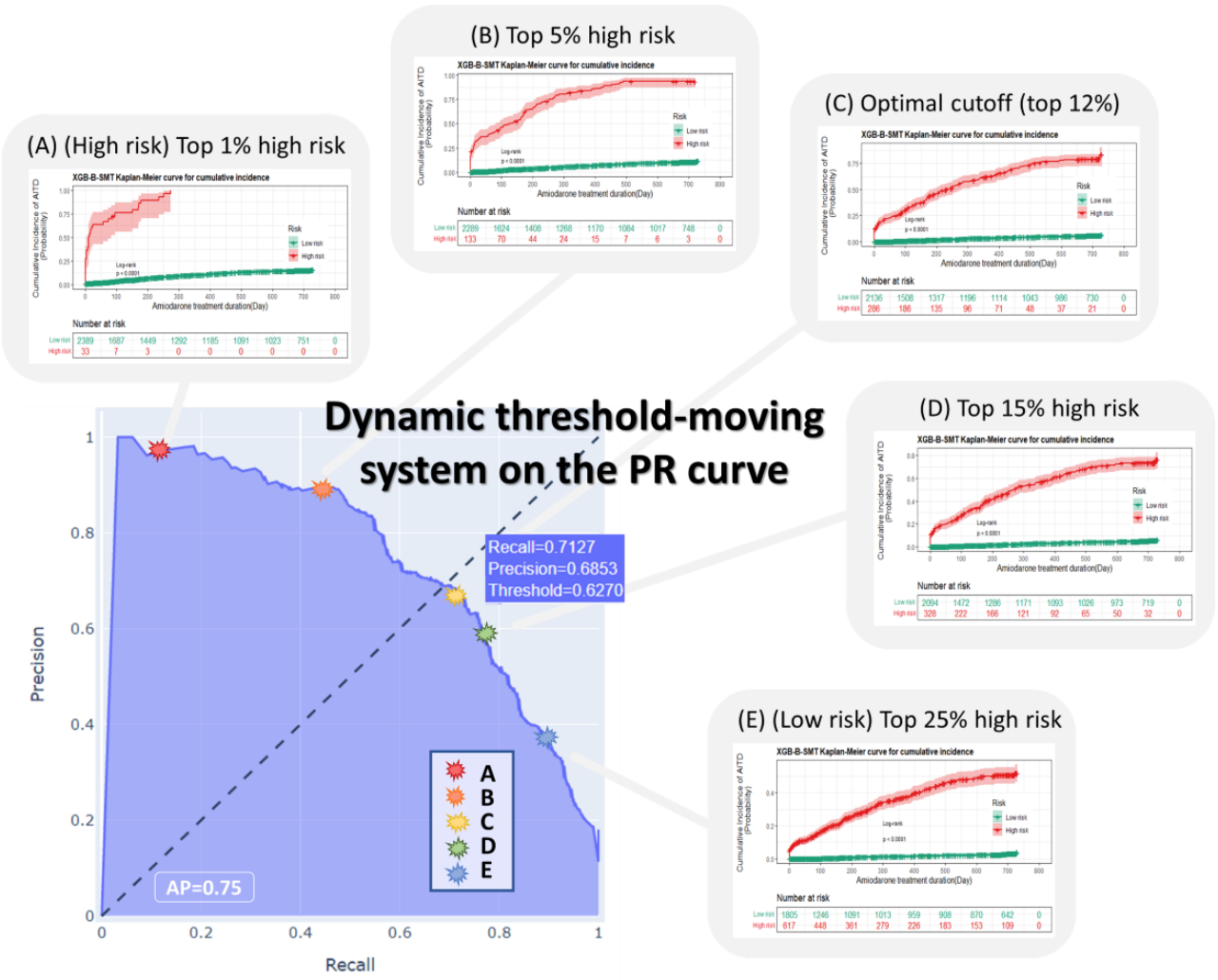

Cutoff	A (High risk)	B	C (Optimal)	D (Default)	E (Low risk)
Top percent	1%	5%	12%	15%	25%
Threshold	0.995	0.953	0.627	0.500	0.142
F_1-score	0.207	0.584	0.699	0.690	0.542
Recall	0.116	0.433	0.713	0.756	0.880
Specificity	1.000	0.993	0.958	0.944	0.825
Precision (PPV)	0.970	0.895	0.685	0.634	0.392
NPV	0.898	0.932	0.963	0.968	0.982

Prediction Distribution

Figure 5 visualizes the prediction distribution of AITD for the 2422 subjects in the external test set. A color change from blue to red indicates increased predicted risk, with a dramatic change occurring around the cutoff point of 0.627. Among 275 patients who developed AITD, 196 (71.3%) had a predicted risk above 0.627 and were determined to be at high risk of AITD according to the XGBoost-borderline SMOTE model. Among the remaining 2147 non-AITD patients, 2057 (95.8%) had a predicted risk lower than the optimal threshold and were thus true negatives estimated by the model.

Figure 5. Prediction distribution of adverse thyroid effects in amiodarone users. Patients were sorted in order of risk; red dots represent the AITD group, while blue dots represent the non-AITD group. AITD: amiodarone-induced thyroid dysfunction.

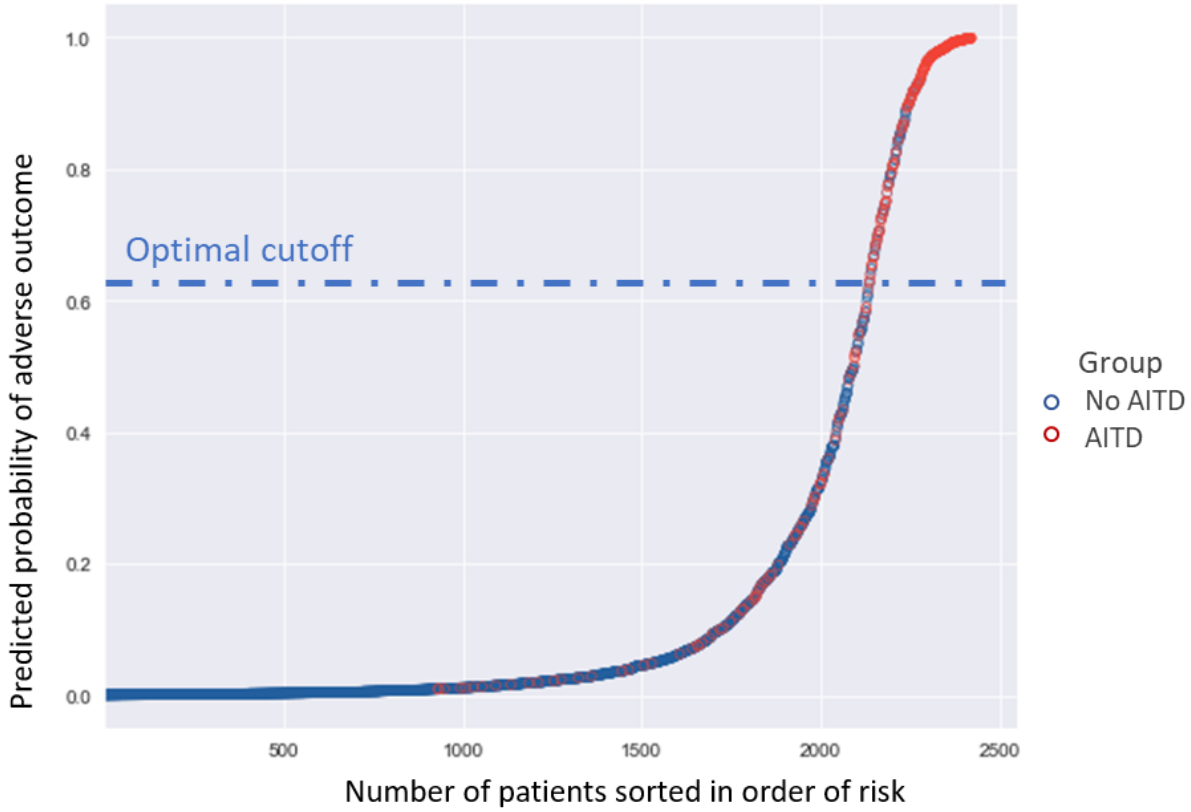

Discussion

Main Findings

This study constructed an explainable and threshold-modifiable machine learning model with the resampling method for AITD risk stratification using dynamic clinical features from the Taipei Medical University clinical research database. The model with the best prediction performance, XGBoost-borderline SMOTE, was validated using external data from another hospital to ensure the credibility and generalizability of the results. It remained robust under conditions of different physicians; Prescription patterns, and hospitals. Resampling methods effectively tackled the imbalanced data and enhanced the model performance. There were 19 clinical features selected by the RFE. Time-series input for dynamic clinical features allowed for real-time assessment and prediction according to a patient's changing disease state. The SHAP plot provided a better visualization tool to understand the contributions of features to AITD. Modifying the threshold on the PR curve by comparison to the KM curve could improve the help provided for clinical decision-making by determining the percentage of the AITD risk population in different practice settings.

Best-Performing Model

The outstanding performance of XGBoost-borderline SMOTE in this study resulted from ensemble learning boosting algorithms and a resampling-oversampling technique. As a tree-based ensemble learning algorithm, XGBoost has been shown to be able to detect the complex and potentially nonlinear relationships in imbalance classification, such as in predicting adverse outcomes of chronic heart failure or the adverse effects of analgesics for osteoarthritis [37,54]. In contrast, KNN was sensitive to the majority of instances and thus performed poorly for imbalance classification [55], while the traditional LR model led to biased parameter estimates and classification performance and was less suitable for handling imbalanced data [55-57]. Interestingly, the study also found that oversampling B-SMT consistently outperformed undersampling ENN and hybrid sampling B-SMT-ENN on AUPRC, recall, and G-mean. The undersampling ENN and hybrid sampling methods used a process that deletes samples from the majority class; therefore, valuable information determining the decision boundary between the classes might have been lost. Borderline SMOTE created synthetic data only along the decision boundary, which was the best-performing strategy in this study; it has previously been used to successfully predict chronic kidney disease and hepatitis B virus infection with class imbalance [58,59].

Feature Identification and Interpretation

This study used SHAP for model interpretation, which allowed precise ranking of variables with clinical reasoning and justification. Top features, such as a high TSH level, short treatment duration, low FT4 level, advanced age, and a higher cumulative amiodarone dose, have been well explained by previous epidemiological studies [6,7,16]. Low alkaline phosphatase and high alanine aminotransferase levels were also found to be associated with hypothyroidism [60]. However, HDL and LDL, which were selected by RFE in this research, were not statistically significantly correlated with thyroid

function in previous pharmacoepidemiological reports [61]. Their contributions might be masked by factorial interactions in statistical approaches. Similar phenomena were reported for thyroid disease, chronic kidney disease, and analgesic adverse-effect prediction [54,62,63]. The machine learning models identified relevant features with nonlinear relationships and complex interactions between factors and outcomes, such as HDL and LDL, in the present study; Promising to help doctors and pharmacists to pay special attention when checking amiodarone users' lipid panels to prevent adverse thyroid events.

Threshold-Moving System on the PR Curve

This study used a moving threshold system on the PR curve to select optimal cutoff points for assessments with the KM curve. This innovative approach not only allowed comparisons of model performance at different decision thresholds, but also further ensured the capability of the model to differentiate clinically significant high- and low-risk groups. As decision threshold adjustment is a known strategy to deal with imbalanced classification, the best cutoff was based on the maximum F_1-score, as in a previous study of diabetes risk prediction [64]. Selecting an extremely low threshold allows capture of all potential AITD events, but a high false alarm rate can overwhelm clinicians. Conversely, an extremely high decision threshold can greatly reduce the false alarm rate with the cost of failing to detect AITD cases. With an unequal class distribution and high misclassification costs in adverse effect predictions, this study will increase attention paid to future studies to determine the optimal threshold based on the maximum F_1-score with a threshold-moving approach and a KM curve to ensure differentiation ability and clinical justification, rather than using the default cutoff (0.5) directly provided by the machine learning software.

Clinical Implications

This machine learning model could be used as a clinical decision-making aid for the early and real-time prediction of AITD by incorporating it into computerized physician order entry systems to optimize amiodarone use. This study collected patients' time-series data to build the model, giving it the capability to provide assessment not only of new amiodarone users but also patients who have used amiodarone for a long time. Patients' disease status changes over time, so only dynamically analyzing the cumulative dose, duration of therapy, and changes in multiple recent laboratory data will enable simultaneous surveillance. The present model does not provide a one-time glimpse of patient status, but a long-term, real-time prediction. Previous studies that used time-series concepts for intradialytic adverse-event risk prediction also provide evidence for this methodology, as their models had better prediction performance than models lacking features extracted from time-series data [65-67]. Using a threshold-moving system on the PR curve allowed us to further visualize threshold adjustments, balancing high noise and the cost of missing cases for clinical consideration. The model in this study should increase the safety of amiodarone use by enabling individualized risk prediction of AITD.

Limitations

The study used the Taipei Medical University clinical research database, incorporating data from 3 hospitals in Taiwan. This database provided detailed clinical information, such as laboratory results, cause of death, and time-points for each medical treatment; it has previously been used to successfully predict mortality or classify patients with end-stage liver disease [68]. However, the study was potentially affected by the loss to follow-up of patients, unrecorded disease status, or unrecorded medications due to its nature as a retrospective data analysis. Family history, genetic data, and dietary intake were not documented in the database, but these factors might be integral to the occurrence of AITD. Extrapolation of the study model is thus restricted. Future multicenter, multicountry data are needed to further train and test the model before applying it in a broader clinical setting.

Conclusions

This study found that XGBoost with the borderline SMOTE resampling technique achieved the best model performance to predict AITD among amiodarone users. Feature selection by RFE and interpretation by SHAP demonstrated good predictive abilities and an explainable model. The optimal point of the threshold was determined to be the one with the maximal F_1-score, found by moving the threshold on the PR curve and differentiating risk groups assessed by the Kaplan-Meier curve. This time-series predictive model can serve as a preliminary tool to support clinicians with individualized AITD risk stratification among amiodarone users.

Data Availability

The data were obtained from the Taipei Medical University clinical research database; this was approved by the Institutional Review Board of Taipei Medical University (TMU-JIRB-N202107054). Data availability is restricted because of the personal information protection requirement of the institutional review board, but the data are available from the corresponding author on reasonable request.

Conflicts of Interest

None declared.

Multimedia Appendix 1

Definition of preexisting thyroid conditions.
[DOCX File , 38 KB-Multimedia Appendix 1]

Multimedia Appendix 2

The eligible data collection period and the details of the time-series data collection diagram.
[DOCX File , 254 KB-Multimedia Appendix 2]

Multimedia Appendix 3

Codebook and missing rate of the features in the study.
[DOCX File , 48 KB-Multimedia Appendix 3]

Multimedia Appendix 4

Hyperparameters combinations in a grid search and final best hyperparameters.
[DOCX File , 43 KB-Multimedia Appendix 4]

Multimedia Appendix 5

Pseudocode for grid search, recursive feature elimination (RFE), and five-fold cross-validation.
[DOCX File , 38 KB-Multimedia Appendix 5]

Multimedia Appendix 6

The formulas of each evaluation metrics and confusion matrix.
[DOCX File , 38 KB-Multimedia Appendix 6]

Multimedia Appendix 7

The STROBE flowchart of patient selection. WFH: Wan Fang Hospital; TMUH: Taipei Medical University Hospital; SHH: Shuang Ho Hospital; labs: laboratory.
[DOCX File , 226 KB-Multimedia Appendix 7]

Multimedia Appendix 8

Recursive feature elimination with five-fold cross-validation (RFECV) feature selection.
[DOCX File , 96 KB-Multimedia Appendix 8]

Multimedia Appendix 9

The training set model performance of accuracy, precision, recall, and F1 score for the raw and resampling methods by 16 machine learning models.
[DOCX File , 46 KB-Multimedia Appendix 9]

Multimedia Appendix 10

Statistical significances of AUPRCs.
[DOCX File , 41 KB-Multimedia Appendix 10]

References

1. Park H, Kim Y. Adverse effects of long-term amiodarone therapy. Korean J Intern Med 2014 Sep;29(5):571-573 [FREE Full text] [doi: 10.3904/kjim.2014.29.5.571] [Medline: 25228830]
2. Goldschlager N, Epstein AE, Naccarelli GV, Olshansky B, Singh B, Collard HR, Practice Guidelines Sub-committee, North American Society of Pacing and Electrophysiology (HRS). A practical guide for clinicians who treat patients with amiodarone: 2007. Heart Rhythm 2007 Sep;4(9):1250-1259. [doi: 10.1016/j.hrthm.2007.07.020] [Medline: 17765636]
3. Kirchhof P, Benussi S, Kotecha D, Ahlsson A, Atar D, Casadei B, ESC Scientific Document Group. 2016 ESC Guidelines for the management of atrial fibrillation developed in collaboration with EACTS. Eur Heart J 2016 Oct 07;37(38):2893-2962 [FREE Full text] [doi: 10.1093/eurheartj/ehw210] [Medline: 27567408]
4. Siddoway L. Amiodarone: guidelines for use and monitoring. Am Fam Physician 2003 Dec 01;68(11):2189-2196 [FREE Full text] [Medline: 14677664]
5. Loh K. Amiodarone-induced thyroid disorders: a clinical review. Postgrad Med J 2000 Mar;76(893):133-140 [FREE Full text] [doi: 10.1136/pmj.76.893.133] [Medline: 10684321]
6. Huang C, Chen P, Chang J, Huang D, Chang S, Chen S, et al. Amiodarone-induced thyroid dysfunction in Taiwan: a retrospective cohort study. Int J Clin Pharm 2014 Apr;36(2):405-411. [doi: 10.1007/s11096-013-9910-9] [Medline: 24515549]

7. Lee KF, Lee KM, Fung TT. Amiodarone-induced thyroid dysfunction in the Hong Kong Chinese population. Hong Kong Med J 2010 Dec;16(6):434-439 [FREE Full text] [Medline: 21135419]
8. Trip MD, Wiersinga W, Plomp TA. Incidence, predictability, and pathogenesis of amiodarone-induced thyrotoxicosis and hypothyroidism. Am J Med 1991 Nov;91(5):507-511. [doi: 10.1016/0002-9343(91)90187-3] [Medline: 1951413]
9. Trohman RG, Sharma PS, McAninch EA, Bianco AC. Amiodarone and thyroid physiology, pathophysiology, diagnosis and management. Trends Cardiovasc Med 2019 Jul;29(5):285-295 [FREE Full text] [doi: 10.1016/j.tcm.2018.09.005] [Medline: 30309693]
10. Bartalena L, Bogazzi F, Chiovato L, Hubalewska-Dydejczyk A, Links T, Vanderpump M. 2018 European Thyroid Association (ETA) Guidelines for the Management of Amiodarone-Associated Thyroid Dysfunction. Eur Thyroid J 2018 Mar;7(2):55-66 [FREE Full text] [doi: 10.1159/000486957] [Medline: 29594056]
11. Kashima A, Funahashi M, Fukumoto K, Komamura K, Kamakura S, Kitakaze M, et al. Pharmacokinetic characteristics of amiodarone in long-term oral therapy in Japanese population. Biol Pharm Bull 2005 Oct;28(10):1934-1938 [FREE Full text] [doi: 10.1248/bpb.28.1934] [Medline: 16204949]
12. Pollak P, Bouillon T, Shafer SL. Population pharmacokinetics of long-term oral amiodarone therapy. Clin Pharmacol Ther 2000 Jun;67(6):642-652. [doi: 10.1067/mcp.2000.107047] [Medline: 10872646]
13. Vassallo P, Trohman RG. Prescribing amiodarone: an evidence-based review of clinical indications. JAMA 2007 Sep 19;298(11):1312-1322. [doi: 10.1001/jama.298.11.1312] [Medline: 17878423]
14. Connolly SJ. Evidence-based analysis of amiodarone efficacy and safety. Circulation 1999 Nov 09;100(19):2025-2034. [doi: 10.1161/01.cir.100.19.2025] [Medline: 10556230]
15. Martino E, Aghini-Lombardi F, Mariotti S, Bartalena L, Lenziardi M, Ceccarelli C, et al. Amiodarone iodine-induced hypothyroidism: risk factors and follow-up in 28 cases. Clin Endocrinol (Oxf) 1987 Feb;26(2):227-237. [doi: 10.1111/j.1365-2265.1987.tb00781.x] [Medline: 3665117]
16. Ahmed S, Van Gelder IC, Wiesfeld ACP, Van Veldhuisen DJ, Links TP. Determinants and outcome of amiodarone-associated thyroid dysfunction. Clin Endocrinol (Oxf) 2011 Sep;75(3):388-394. [doi: 10.1111/j.1365-2265.2011.04087.x] [Medline: 21535072]
17. Zosin I, Balaş M. Amiodarone-induced thyroid dysfunction in an iodine-replete area: epidemiological and clinical data. Endokrynol Pol 2012;63(1):2-9. [Medline: 22378090]
18. Zhong B, Wang Y, Zhang G, Wang Z. Environmental iodine content, female sex and age are associated with new-onset amiodarone-induced hypothyroidism: a systematic review and meta-analysis of adverse reactions of amiodarone on the thyroid. Cardiology 2016;134(3):366-371. [doi: 10.1159/000444578] [Medline: 27100205]
19. Thorne SA, Barnes I, Cullinan P, Somerville J. Amiodarone-associated thyroid dysfunction: risk factors in adults with congenital heart disease. Circulation 1999 Jul 13;100(2):149-154. [doi: 10.1161/01.cir.100.2.149] [Medline: 10402444]
20. Basaria S, Cooper DS. Amiodarone and the thyroid. Am J Med 2005 Jul;118(7):706-714. [doi: 10.1016/j.amjmed.2004.11.028] [Medline: 15989900]
21. Martino E, Safran M, Aghini-Lombardi F, Rajatanavin R, Lenziardi M, Fay M, et al. Environmental iodine intake and thyroid dysfunction during chronic amiodarone therapy. Ann Intern Med 1984 Jul;101(1):28-34. [doi: 10.7326/0003-4819-101-1-28] [Medline: 6428291]
22. Tsadok MA, Jackevicius CA, Rahme E, Essebag V, Eisenberg MJ, Humphries KH, et al. Amiodarone-induced thyroid dysfunction: brand-name versus generic formulations. CMAJ 2011 Sep 06;183(12):E817-E823 [FREE Full text] [doi: 10.1503/cmaj.101800] [Medline: 21746822]
23. Stan MN, Hess EP, Bahn RS, Warnes CA, Ammash NM, Brennan MD, et al. A risk prediction index for amiodarone-induced thyrotoxicosis in adults with congenital heart disease. J Thyroid Res 2012;2012:210529 [FREE Full text] [doi: 10.1155/2012/210529] [Medline: 22518347]
24. Kinoshita S, Hayashi T, Wada K, Yamato M, Kuwahara T, Anzai T, et al. Risk factors for amiodarone-induced thyroid dysfunction in Japan. J Arrhythm 2016 Dec;32(6):474-480 [FREE Full text] [doi: 10.1016/j.joa.2016.03.008] [Medline: 27920832]
25. Uchida T, Kasai T, Takagi A, Sekita G, Komiya K, Takeno K, et al. Prevalence of amiodarone-induced thyrotoxicosis and associated risk factors in Japanese patients. Int J Endocrinol 2014;2014:534904 [FREE Full text] [doi: 10.1155/2014/534904] [Medline: 25053942]
26. Fischer AJ, Enders D, Eckardt L, Köbe J, Wasmer K, Breithardt G, et al. Thyroid dysfunction under amiodarone in patients with and without congenital heart disease: results of a nationwide analysis. J Clin Med 2022 Apr 05;11(7):2027 [FREE Full text] [doi: 10.3390/jcm11072027] [Medline: 35407633]
27. Kim W, Cho Y, Kim D, Jo A, Min K, Lee K. Factors associated with thyroid-related adverse events in patients receiving PD-1 or PD-L1 inhibitors using machine learning models. Cancers (Basel) 2021 Oct 30;13(21):5465 [FREE Full text] [doi: 10.3390/cancers13215465] [Medline: 34771631]
28. Chowdhury MZI, Naeem I, Quan H, Leung AA, Sikdar KC, O'Beirne M, et al. Prediction of hypertension using traditional regression and machine learning models: A systematic review and meta-analysis. PLoS One 2022;17(4):e0266334 [FREE Full text] [doi: 10.1371/journal.pone.0266334] [Medline: 35390039]

29. Liew BXW, Kovacs FM, Rügamer D, Royuela A. Machine learning versus logistic regression for prognostic modelling in individuals with non-specific neck pain. Eur Spine J 2022 Aug;31(8):2082-2091. [doi: 10.1007/s00586-022-07188-w] [Medline: 35353221]
30. Singal A, Mukherjee A, Elmunzer BJ, Higgins PDR, Lok AS, Zhu J, et al. Machine learning algorithms outperform conventional regression models in predicting development of hepatocellular carcinoma. Am J Gastroenterol 2013 Nov;108(11):1723-1730 [FREE Full text] [doi: 10.1038/ajg.2013.332] [Medline: 24169273]
31. Zhang P, Jia Y, Shang Y. Research and application of XGBoost in imbalanced data. Int J Distrib Sens Netw 2022 Jun 29;18(6):155013292211069 [FREE Full text] [doi: 10.1177/15501329221106935]
32. Wang W, Sun D. The improved AdaBoost algorithms for imbalanced data classification. Inf Sci 2021 Jul;563:358-374. [doi: 10.1016/j.ins.2021.03.042]
33. Nair P. Optimization of kNN Classifier Using Hybrid Preprocessing Model for Handling Imbalanced Data. Research India Publications. 2019. URL: https://www.ripublication.com/irph/ijert19/ijertv12n5_17.pdf [accessed 2023-01-19]
34. Ishaq A, Sadiq S, Umer M, Ullah S, Mirjalili S, Rupapara V, et al. Improving the Prediction of Heart Failure Patients' Survival Using SMOTE and Effective Data Mining Techniques. IEEE Access 2021;9:39707-39716 [FREE Full text] [doi: 10.1109/access.2021.3064084]
35. Zhang S, Yuan Y, Yao Z, Wang X, Lei Z. Improvement of the performance of models for predicting coronary artery disease based on XGBoost algorithm and feature processing technology. Electronics 2022 Jan 20;11(3):315 [FREE Full text] [doi: 10.3390/electronics11030315]
36. Wang K, Adrian AM, Chen K, Wang K. A hybrid classifier combining Borderline-SMOTE with AIRS algorithm for estimating brain metastasis from lung cancer: a case study in Taiwan. Comput Methods Programs Biomed 2015 Apr;119(2):63-76. [doi: 10.1016/j.cmpb.2015.03.003] [Medline: 25823851]
37. Wang K, Tian J, Zheng C, Yang H, Ren J, Li C, et al. Improving risk identification of adverse outcomes in chronic heart failure using SMOTE+ENN and machine learning. Risk Manag Healthc Policy 2021;14:2453-2463 [FREE Full text] [doi: 10.2147/RMHP.S310295] [Medline: 34149290]
38. Decaro C, Montanari GB, Bianconi M, Bellanca G. Prediction of hematocrit through imbalanced dataset of blood spectra. Healthc Technol Lett 2021 Apr;8(2):37-44 [FREE Full text] [doi: 10.1049/htl2.12006] [Medline: 33850628]
39. Vepa A, Saleem A, Rakhshan K, Daneshkhah A, Sedighi T, Shohaimi S, et al. Using machine learning algorithms to develop a clinical decision-making tool for COVID-19 inpatients. Int J Environ Res Public Health 2021 Jun 09;18(12):6228 [FREE Full text] [doi: 10.3390/ijerph18126228] [Medline: 34207560]
40. Collins GS, Reitsma JB, Altman DG, Moons K. Transparent reporting of a multivariable prediction model for individual prognosis or diagnosis (TRIPOD): the TRIPOD Statement. BMC Med 2015 Jan 06;13:1 [FREE Full text] [doi: 10.1186/s12916-014-0241-z] [Medline: 25563062]
41. Pedregosa F. Scikit-learn: machine learning in Python. J Mach Learn Res 2011;12:2022-2010 [FREE Full text]
42. Thorsen-Meyer H, Nielsen AB, Nielsen AP, Kaas-Hansen BS, Toft P, Schierbeck J, et al. Dynamic and explainable machine learning prediction of mortality in patients in the intensive care unit: a retrospective study of high-frequency data in electronic patient records. Lancet Digit Health 2020 Apr;2(4):e179-e191 [FREE Full text] [doi: 10.1016/S2589-7500(20)30018-2] [Medline: 33328078]
43. Hu Z, Melton GB, Arsoniadis EG, Wang Y, Kwaan MR, Simon GJ. Strategies for handling missing clinical data for automated surgical site infection detection from the electronic health record. J Biomed Inform 2017 Apr;68:112-120 [FREE Full text] [doi: 10.1016/j.jbi.2017.03.009] [Medline: 28323112]
44. van Buuren S, Oudshoorn CGM. Multivariate Imputation by Chained Equations: MICE v1 User's Manual. stefvanbuuren.name. 2000. URL: https://stefvanbuuren.name/publications/MICE%20V1.0%20Manual%20TNO00038%202000.pdf [accessed 2023-01-19]
45. Isaacs M, Costin M, Bova R, Barrett HL, Heffernan D, Samaras K, et al. Management of amiodarone-induced thyrotoxicosis at a cardiac transplantation centre. Front Endocrinol (Lausanne) 2018;9:482 [FREE Full text] [doi: 10.3389/fendo.2018.00482] [Medline: 30186240]
46. Han H, Wang WY, Mao BH. Advances in intelligent computing. In: Huang DS, Zhang XP, Huang GB, editors. ICIC 2005. Lecture Notes in Computer Science, vol 3644. Berlin, Germany: Springer; 2005.
47. Beckmann M, Ebecken NFF, Pires de Lima BSL. A KNN undersampling approach for data balancing. JILSA 2015;7(04):104 [FREE Full text] [doi: 10.4236/jilsa.2015.74010]
48. Bekkar M. Evaluation measures for models assessment over imbalanced data sets. Journal of Information Engineering and Applications 2013;3:2022-2010 [FREE Full text]
49. Brabec J, Komárek T, Franc V. On model evaluation under non-constant class imbalance. In: Computational Science – ICCS 2020. Cham, Switzerland: Springer; 2020.
50. Sofaer HR, Hoeting JA, Jarnevich CS. The area under the precision‐recall curve as a performance metric for rare binary events. Methods Ecol Evol 2019 Feb 14;10(4):565-577 [FREE Full text] [doi: 10.1111/2041-210x.13140]
51. Japkowicz N. Assessment metrics for imbalanced learning. In: Haibo H, Yunqian M, editors. Imbalanced Learning: Foundations, Algorithms, and Applications. Hoboken, NJ: Wiley; 2013:187-206.

52. Lundberg S, Lee SI. A unified approach to interpreting model predictions. 2017 Presented at: 31st Conference on Neural Information Processing Systems (NIPS 2017); Dec 4-9, 2017; Long Beach, CA p. 2022-2010 URL: https://dl.acm.org/doi/pdf/10.5555/3295222.3295230
53. Lipton ZC, Elkan C, Naryanaswamy B. Optimal Thresholding of Classifiers to Maximize F1 Measure. In: Calders T, Esposito F, Hüllermeier E, editors. Machine Learning and Knowledge Discovery in Databases. ECML PKDD 2014. Lecture Notes in Computer Science, vol 8725. Berlin, Germany: Springer; 2014.
54. Liu L, Yu Y, Fei Z, Li M, Wu F, Li H, et al. An interpretable boosting model to predict side effects of analgesics for osteoarthritis. BMC Syst Biol 2018 Nov 22;12(Suppl 6):105 [FREE Full text] [doi: 10.1186/s12918-018-0624-4] [Medline: 30463545]
55. Louzada F, Ara A, Fernandes GB. Classification methods applied to credit scoring: Systematic review and overall comparison. Surv Oper Res Manag Sci 2016 Dec;21(2):117-134. [doi: 10.1016/j.sorms.2016.10.001]
56. Owen A. Infinitely imbalanced logistic regression. J Mach Learn Res 2007;8(4):761-773 [FREE Full text]
57. Yazhe L, Tony B, Niall A. Issues using logistic regression with class imbalance, with a case study from credit risk modelling. Found Data Sci 2019;1(4):389-417 [FREE Full text] [doi: 10.3934/fods.2019016]
58. Silveira ACMD, Sobrinho Á, Silva LDD, Costa EDB, Pinheiro ME, Perkusich A. Exploring early prediction of chronic kidney disease using machine learning algorithms for small and imbalanced datasets. Appl Sci 2022 Apr 06;12(7):3673 [FREE Full text] [doi: 10.3390/app12073673]
59. Wang Y, Du Z, Lawrence WR, Huang Y, Deng Y, Hao Y. Predicting hepatitis B virus infection based on health examination data of community population. Int J Environ Res Public Health 2019 Dec 02;16(23):4842 [FREE Full text] [doi: 10.3390/ijerph16234842] [Medline: 31810204]
60. Al-Janabi G, Hassan HN, Al-Fahham A. Biochemical changes in patients during hypothyroid phase after thyroidectomy. J Med Life 2022 Jan;15(1):104-108 [FREE Full text] [doi: 10.25122/jml-2021-0297] [Medline: 35186143]
61. Cheng X, Li S, Deng L, Luo W, Wang D, Cheng J, et al. Predicting elevated TSH levels in the physical examination population with a machine learning model. Front Endocrinol (Lausanne) 2022;13:839829 [FREE Full text] [doi: 10.3389/fendo.2022.839829] [Medline: 35282438]
62. Wang W, Chakraborty G, Chakraborty B. Predicting the risk of chronic kidney disease (CKD) using machine learning algorithm. Appl Sci 2020 Dec 28;11(1):202 [FREE Full text] [doi: 10.3390/app11010202]
63. Islam S, Haque MS, Miah MSU, Sarwar TB, Nugraha R. Application of machine learning algorithms to predict the thyroid disease risk: an experimental comparative study. PeerJ Comput Sci 2022;8:e898 [FREE Full text] [doi: 10.7717/peerj-cs.898] [Medline: 35494828]
64. Sadeghi S, Khalili D, Ramezankhani A, Mansournia MA, Parsaeian M. Diabetes mellitus risk prediction in the presence of class imbalance using flexible machine learning methods. BMC Med Inform Decis Mak 2022 Feb 10;22(1):36 [FREE Full text] [doi: 10.1186/s12911-022-01775-z] [Medline: 35139846]
65. Liu Y, Yang C, Chiu P, Lin H, Lo C, Lai AS, et al. Machine learning analysis of time-dependent features for predicting adverse events during hemodialysis therapy: model development and validation. J Med Internet Res 2021 Sep 07;23(9):e27098 [FREE Full text] [doi: 10.2196/27098] [Medline: 34491204]
66. Gabutti L, Vadilonga D, Mombelli G, Burnier M, Marone C. Artificial neural networks improve the prediction of Kt/V, follow-up dietary protein intake and hypotension risk in haemodialysis patients. Nephrol Dial Transplant 2004 May;19(5):1204-1211. [doi: 10.1093/ndt/gfh084] [Medline: 14993478]
67. Gabutti L, Machacek M, Marone C, Ferrari P. Predicting intradialytic hypotension from experience, statistical models and artificial neural networks. J Nephrol 2005;18(4):409-416. [Medline: 16245245]
68. Lin Y, Chen R, Tang J, Yu C, Wu JL, Chen L, et al. Machine-learning monitoring system for predicting mortality among patients with noncancer end-stage liver disease: retrospective study. JMIR Med Inform 2020 Oct 30;8(10):e24305 [FREE Full text] [doi: 10.2196/24305] [Medline: 33124991]

Abbreviations

AdaBoost: adaptive boosting
AITD: amiodarone-induced thyroid dysfunction
B-SMT: borderline synthetic minority oversampling technique
ENN: edited near neighbors
fT4: free thyroxin
HDL: high-density lipoprotein
ICD: International Classification of Diseases
KM: Kaplan-Meier
KNN: k-nearest neighbor
LDL: low-density lipoprotein
LR: logistic regression
PR: precision-recall

RFE: Recursive feature elimination
RFECV: recursive feature elimination cross-validation
SHAP: Shapley additive explanation
SMOTE: synthetic minority oversampling technique
TSH: thyroid-stimulating hormone
XGBoost: extreme gradient boosting

Edited by G Eysenbach; submitted 25.10.22; peer-reviewed by T Yang, Y Guo; comments to author 06.12.22; revised version received 25.12.22; accepted 16.01.23; published 07.02.23

Please cite as:
Lu YT, Chao HJ, Chiang YC, Chen HY
Explainable Machine Learning Techniques To Predict Amiodarone-Induced Thyroid Dysfunction Risk: Multicenter, Retrospective Study With External Validation
J Med Internet Res 2023;25:e43734
URL: https://www.jmir.org/2023/1/e43734
doi: 10.2196/43734
PMID: 36749620